IMMUNE TOLERANCE

Regulatory T cells generated early in life play a distinct role in maintaining self-tolerance

Siyoung Yang,[1,2]* Noriyuki Fujikado,[1]* Dmitriy Kolodin,[1] Christophe Benoist,[1,3]† Diane Mathis[1,3]†

Aire is an important regulator of immunological tolerance, operating in a minute subset of thymic stromal cells to induce transcripts encoding peptides that guide T cell selection. Expression of Aire during a perinatal age window is necessary and sufficient to prevent the multiorgan autoimmunity characteristic of Aire-deficient mice. We report that Aire promotes the perinatal generation of a distinct compartment of $Foxp3^+CD4^+$ regulatory T (T_{reg}) cells, which stably persists in adult mice. This population has a role in maintaining self-tolerance, a transcriptome and an activation profile distinguishable from those of T_{regs} produced in adults. Underlying the distinct T_{reg} populations are age-dependent, Aire-independent differences in the processing and presentation of thymic stromal-cell peptides, resulting in different T cell receptor repertoires. Our findings expand the notion of a developmentally layered immune system.

Individuals with APECED (autoimmune polyendocrinopathy–candidiasis–ectodermal dystrophy) have a mutation in the gene encoding Aire. Such individuals, and mice lacking Aire, develop multiorgan autoimmune disease. Aire promotes immunological tolerance by inducing, specifically in thymic medullary epithelial cells (MECs), a large repertoire of mRNA transcripts encoding proteins characteristic of differentiated cell types (peripheral-tissue antigens, PTAs), such as insulin or casein-α. Peptides derived from these proteins are displayed on major histocompatibility complex (MHC) molecules at the MEC surface. The MHC:PTA-peptide complexes negatively select thymocytes whose antigen (Ag) receptors (T cell receptors, TCRs) are engaged too avidly. In addition, MECs can positively select $Foxp3^+CD4^+$ regulatory T (T_{reg}) cells (*1*, *2*), at least some of them in an Aire-dependent manner (*3*, *4*). Cross-presentation of Aire-induced PTAs by thymic dendritic cells (DCs) also occurs and can promote either negative or positive selection (*4*, *5*). Aire's presence during the first few weeks of life is necessary and sufficient to guard against the autoimmune disease characteristic of *Aire*-knockout (KO) mice (*6*). We sought to uncover the root of this unexpected finding.

To compare the effectiveness of clonal deletion in perinatal and adult mice, we examined the thymus of young and old *Aire*-WT (wild-type) and *Aire*-KO animals expressing (i) membrane-bound ovalbumin driven by the rat insulin promoter (RIP-mOva), and thereby within MECs; and (ii) TCRs that recognize a peptide of ovalbumin presented by MHC-II molecules (OT-II) (*7*, *8*). In both perinatal and adult mice, Aire-dependent clonal deletion was readily evident (fig. S1).

As a first step in comparing the T_{reg} compartments, we enumerated $Foxp3^+CD4^+$ T cells in the thymus of progressively older *Aire*-WT and -KO mice (Fig. 1A and fig. S2A). Although a few T_{regs} were detected in the thymus of WT individuals 2 days after birth, a substantial population was evident only on day 4, and it gradually increased through day 35. KO mice showed a similar pattern of T_{reg} accumulation in the thymus, but their fractional representation was reduced relative to WT littermates through day 35, and their numbers until day 10. Results were similar in the periphery (fig. S2, A and B).

To address the relative importance of the T_{reg} compartments for the maintenance of immunological tolerance, we used a NOD.*Foxp3-DTR* system to deplete T_{regs} during the day 0 to 10 or day 35 to 45 age window and followed the mice until 15 weeks of age (or loss of ≥ 20% body weight). Depletion of T_{regs} during the 0- to 10-day window resulted in significant weight reduction by 16 days of age (even though T_{reg} numbers were normal by days 11 to 12) and ≥20% weight loss in all mice by 24 days (Fig. 1B). All individuals showed the multiorgan autoimmunity typical of *Aire*-KO mice on the NOD genetic background (Fig. 1B and fig. S3). In contrast, T_{reg} ablation during the 35- to 45-day window had no significant effect on either weight gain or survival, although there were some mild manifestations of autoimmunity in scattered individuals (figs. S3 and S4).

We next performed a complementation experiment to rule out the trivial explanation that perinatal mice are nonspecifically perturbed by the repeated injection of diphtheria toxin (DT). Addition of T_{regs} from 20-day-old T_{reg}-replete, but not T_{reg}-depleted, donors to recipients perinatally depleted of T_{regs} resulted in a marked improvement in the autoimmune manifestations (figs. S5 and S6). To confirm that the critical perinatally generated T_{reg} population was, indeed, Aire-dependent, we transferred T_{regs} isolated from 20-day-old *Aire*-WT or -KO mice into either T_{reg}-depleted (Fig. 1, C and D) or *Aire*-KO (fig. S7) perinates. For both types of recipient, only the perinatal T_{regs} from WT mice protected against development of the characteristic "Aire-less" autoimmune disease. Thus, Aire promotes the generation of T_{reg} cells during the perinatal age window. Mice lacking these cells phenocopy *Aire*-KO mice; exhibiting a spectrum of pathology that differs substantially from that of mice either constitutively lacking T_{regs} or depleted of them as adults (*9*–*11*).

An inducible T_{reg} lineage-tracer system (*12*) allowed us to explore the functional and phenotypic properties of perinatally generated T_{regs}. In NOD-backcrossed $Foxp3^{eGFP\text{-}Cre\text{-}ERT2}$xR26Y mice, all $Foxp3^+CD4^+$ cells express green fluorescent protein (GFP); treatment with tamoxifen turns on expression of yellow fluorescent protein (YFP) in the T_{regs} extant during drug coverage, rendering them GFP/YFP double-positive thereafter. We first used this system to examine the stability of T_{regs} made perinatally. Lineage-tracer mice were injected with tamoxifen from days 0 to 10 or 35 to 45, and their splenic T_{reg} compartment was analyzed 1 day, 1 week, or 8 weeks later (Fig. 2). The adult-tagged and perinate-tagged T_{reg} populations were both readily discernible the day after termination of tamoxifen, constituting about a quarter of the $Foxp3^+CD4^+$ compartment. For adult-tagged T_{regs}, this fraction remained similar throughout the period examined. In contrast, perinate-tagged T_{regs} dwindled to a minor component of the $Foxp3^+CD4^+$ compartment between 1 and 8 weeks after cessation of labeling. This reduction in fractional representation was a dilution effect as total T_{reg} numbers increased exponentially during this time. Indeed, the actual numbers of perinate-tagged T_{regs} were very stable over the 2 months examined.

The persistence of the tagged T_{reg} populations permitted us to address the functionality of perinatally generated T_{regs} by conducting a four-way comparison (as schematized in fig. S8A). Mice were treated with tamoxifen from 0 to 10 or 35 to 45 days and were then left unmanipulated until 60 days of age, at which time the GFP^+YFP^+ (tagged) T_{reg} and GFP^+YFP^- (bulk) T_{reg} populations were sorted and transferred into newborn *Aire*-KO mice. According to all criteria evaluated, disease was not affected by the introduction of adult-tagged T_{regs} or control bulk T_{reg} population (Fig. 2, B to D, and fig. S8B). In contrast, an addition of perinate-tagged T_{regs} resulted in a substantial reversal of the typical *Aire*-KO pathology (but with substitution of the insulitis characteristic of classical NOD mice) (Fig. 2E and fig. S8B). These findings argue that the T_{reg} population generated perinatally has distinct functional properties that persist within the adult environment.

We also sorted GFP^+YFP^+ and GFP^+YFP^- $CD4^+$ T cells from 8- to 10-week-old mice whose T_{regs}

[1]Division of Immunology, Department of Microbiology and Immunobiology, Harvard Medical School, Boston, MA 02115, USA. [2]Aging Intervention Research Center, Korea Research Institute of Bioscience and Biotechnology (KRIBB), 125 Gwahak-ro, Yuseong-gu, Daejeon, 305-806, South Korea. [3]Evergrande Center for Immunologic Diseases, Harvard Medical School and Brigham and Women's Hospital, Boston MA 02115, USA.
*These authors contributed equally to this work. †Corresponding author. E-mail: cbdm@hms.harvard.edu

had been labeled between 0 and 10 or 35 and 45 days after birth and analyzed their transcriptomes. Distinct sets of genes were either over- (pink) or underexpressed (green) in T_{reg} cells tagged perinatally versus the bulk T_{reg} population of the same mice, but were not differentially transcribed in mice whose T_{regs} were labeled as adults (Fig. 3A and table S1). Overlaying the standard T_{reg} signature on a volcano plot comparing the two labeled T_{reg} populations revealed an overrepresentation of T_{reg} "up" genes in perinate-tagged T_{regs} (Fig. 3B). Indeed, these T_{regs} performed better than the three comparator populations in a typical in vitro suppression assay (Fig. 3C), perhaps reflecting higher transcription of genes, such as *Fgl2*, *Ebi3*, *Pdcd1*, and *Icos* (table S1A), previously implicated in T_{reg} effector function (*13*–*16*). The perinate-tagged T_{reg} population was in a more activated state (Fig. 3D), which fit with its higher content of $CD44^{hi}CD62L^{lo}$ cells (Fig. 3E). It was also more proliferative, as indicated by fractions of EdU-incorporating and of $Ki67^{+}$ cells higher than those of the three comparator populations (Fig. 3F). Indeed, the top pathways overrepresented in perinate-tagged T_{regs} according to Gene-Set Enrichment Analysis (GSEA) were related to DNA replication and cell division (e.g., Fig. 3G). We confirmed the elevated expression of a number of functionally relevant genes at the protein level (Fig. 3H and fig. S9).

Lastly, we sought a molecular or cellular explanation for the distinct T_{reg} compartments generated in perinatal and adult mice. We first used a mixed fetal-liver:bone-marrow chimera approach to rule out the possibility that T cell precursors derived from fetal liver hematopoietic stem cells, which service the developing immune system for the first few weeks after birth (*17*), are predisposed to yield T_{regs} with particular properties, assessing both reconstitution efficiencies and gene-expression profiles (fig. S10).

To facilitate comparison of the repertoires of Aire-dependent PTA transcripts in perinatal and adult MECs, we generated Adig reporter mice, which express GFP under the dictates of *Aire* promoter and enhancer elements (*18*), on either an *Aire*-WT or -KO background. $GFP^{+}MHC\text{-}II^{hi}$ cells were isolated from thymic stroma of <3-day-old or 5-week-old animals, and gene-expression profiling was performed. The fraction of Aire $^{+}MHC\text{-}II^{hi}$ MECs and the Aire mean fluorescence intensity (MFI) were indistinguishable in mice of the two ages (fig. S11, A and B). The repertories of Aire-dependent MEC transcripts were also extremely similar (fig. S11C).

Next, we asked whether the similar repertoires of PTA transcripts might still yield distinct sets of MHC-presented peptides, owing to different Ag-processing and presentation machinery in mice of the two ages, which need not be Aire dependent. Transcripts encoding several molecules implicated in generating or regulating the repertoire of peptides bound to MHC-II or -I molecules were differentially expressed in perinatal

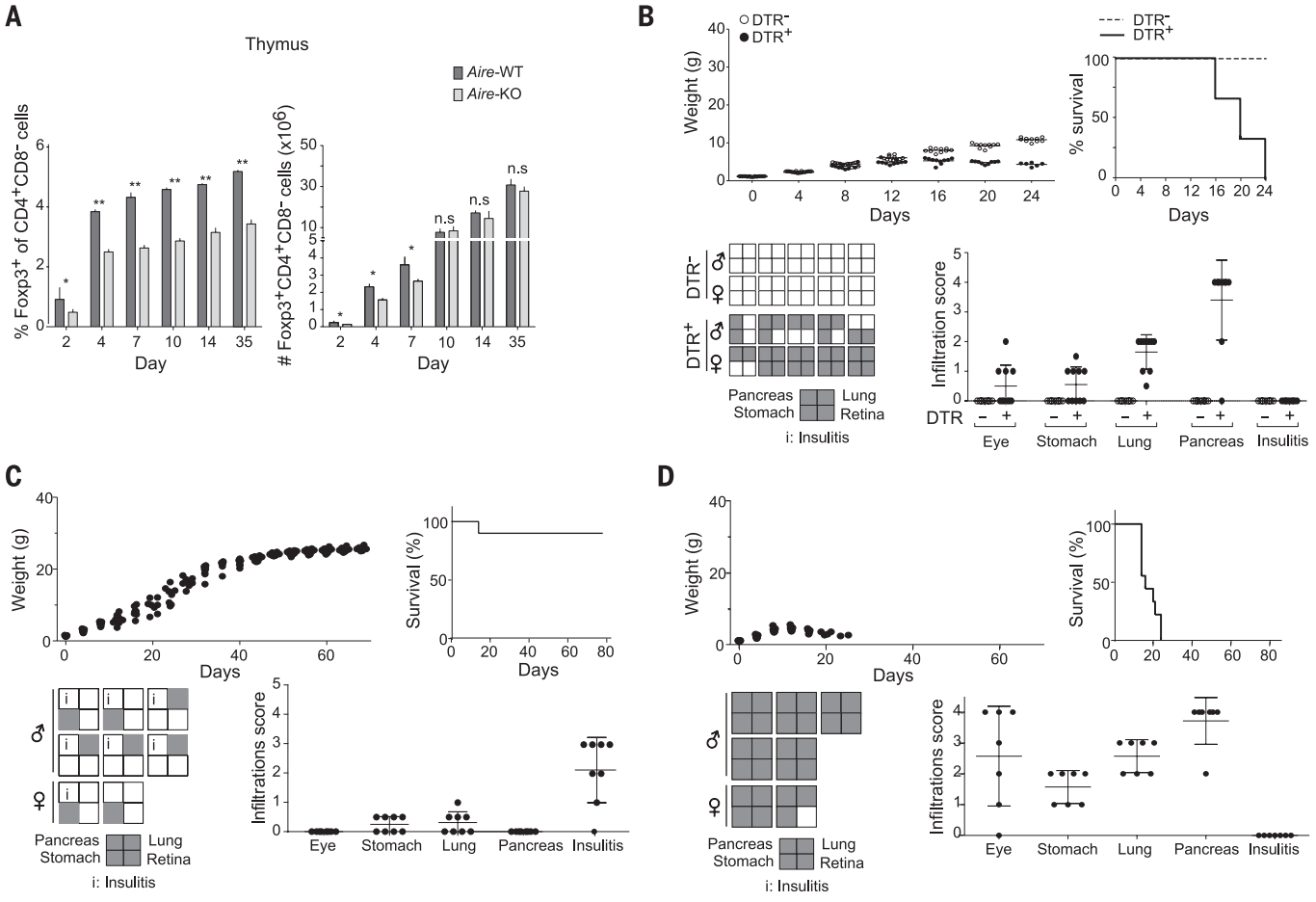

Fig. 1. A perinatal T_{reg} population that is Aire dependent and guards against the autoimmune manifestations typical of *Aire*-KO mice. (**A**) Summary data for fractional representation (left) and numbers (right) of $Foxp3^{+}CD4^{+}CD8^{-}$ thymocytes from *Aire*-WT or -KO mice of increasing age. $^{*}P \leq 0.05$, $^{**}P \leq 0.01$ (Student's *t* test); n.s, not significant; $n = 5$. Examples of corresponding dot-plots can be found in fig. S2A. (**B**) T_{reg} depletion in perinates. Perinatal (0.5 days after birth) NOD.*Foxp3-DTR*$^{+}$ mice or DTR^{-} littermates were treated every other day until day 10 with DT and then followed for manifestations of autoimmune disease. Perinates were examined <24 days after birth because of wasting in the DTR^{+} littermates. Upper left: weight curves. Upper right: survival curves; mice were killed if their weight fell to <20% of that of their DTR^{-} littermates. Lower left: presence (shaded) or absence of organ infiltrates; "i" indicates that insulitis replaced infiltration of the exocrine pancreas. Lower right: severity of organ infiltration (scored as indicated in the supplementary materials and methods). $n = 9$. (**C** and **D**) NOD.*Foxp3.DTR*$^{+}$ mice perinatally depleted of T_{regs} as in (B) were supplemented on days 12 and 19 with T_{regs} isolated from 20-day-old *Aire*-WT (C) or -KO (D) littermates. Cohorts were followed until 70 days of age. $n = 9$. The experimental setup was otherwise the same as in (B).

and adult MECs (Fig. 4A). The data on *H2-O* transcripts drew our attention because DO is known to inhibit the activity of DM, an "editor" needed for dislodging the invariant chain (CD74) derivative, CLIP, and other peptides from the Ag-binding groove of a maturing MHC-II molecule, enabling effective loading of a diverse repertoire of peptides (*19*, *20*). Transcripts encoding both DO chains were expressed at a significantly lower level in perinatal than in adult MECs, independently of Aire (Fig. 4B); perinatal MECs also had reduced amounts of intracellular DO complexes (Fig. 4C). In addition, they displayed higher intracellular amounts of DM complexes (Fig. 4E). Co-plotting intracellular amounts of the two complexes at the single-cell level revealed a subset of perinatal MECs with reduced DO and enhanced DM expression (Fig. 4F). A lower DO:DM ratio should promote more effective replacement of CLIP by other peptides. Indeed, a higher percentage of perinatal MECs displayed low amounts of or no CLIP (37.6 ± 6.4% versus 20.9 ± 2.2%), and the CLIP MFI was lower for perinatal MECs (761.7 ± 78.7%

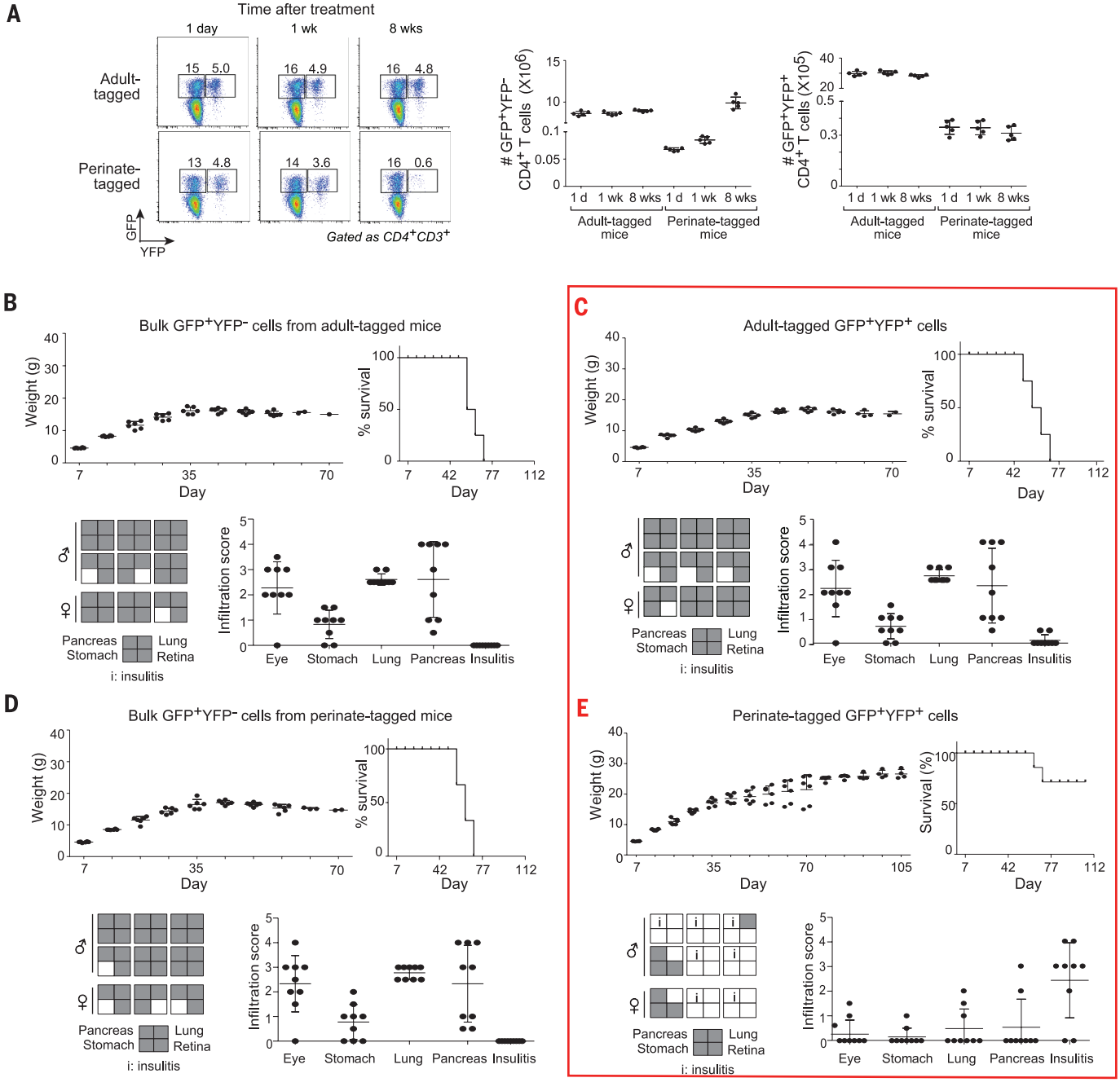

Fig. 2. Stability and function of perinate- versus adult-tagged T_{regs}. (**A**) Tamoxifen was administered from 0 to 10 or 35 to 45 days of age; at various times later, splenocytes were analyzed for GFP and YFP expression by flow cytometry. Left: representative flow-cytometric dot-plots. Numbers represent percentages of $CD4^+3^+$ cells in the designated gates. Center: summary data on numbers of GFP^+YFP^- bulk T_{regs}. Right: corresponding data on GFP^+YFP^+ perinate-tagged or adult-tagged T_{regs} from the same mice. $n = 5$. (**B** to **E**) T_{regs} (1.5×10^5) were transferred into *Aire*-KO mice on days 0.5, 3, and 7 after birth, and the recipients were monitored until 16 weeks of age. A four-way comparison as schematized in fig. S8A: GFP^+YFP^+ T_{regs} tagged from 35 to 45 days of age and isolated from a 60-day-old mouse (C), GFP^+YFP^- bulk T_{regs} from the same mouse (B), GFP^+YFP^+ T_{regs} tagged from 0 to 10 days of age and isolated from a 60-day-old mouse (E), and GFP^+YFP^- bulk T_{regs} from the same mouse (D). Data organized as in Fig. 1B. The key comparison is boxed.

versus 1019.0 ± 54%) (Fig. 4G). Thus, the repertoires of peptides presented by perinatal and adult MECs are different, the latter appearing to be more limited.

Aire-dependent PTAs can be "cross-presented" by myeloid-lineage cells in the vicinity (*4*, *5*), primarily MHC-II^{hi}CD8α^+ DCs (*4*). Interestingly, this cell type was present in strongly reduced amounts in thymi from perinatal mice (Fig. 4H). Because the splenic MHC-II^{hi}CD8α^+ DC subset showed an even more extreme age dependence, it is unlikely that this difference is Aire dependent.

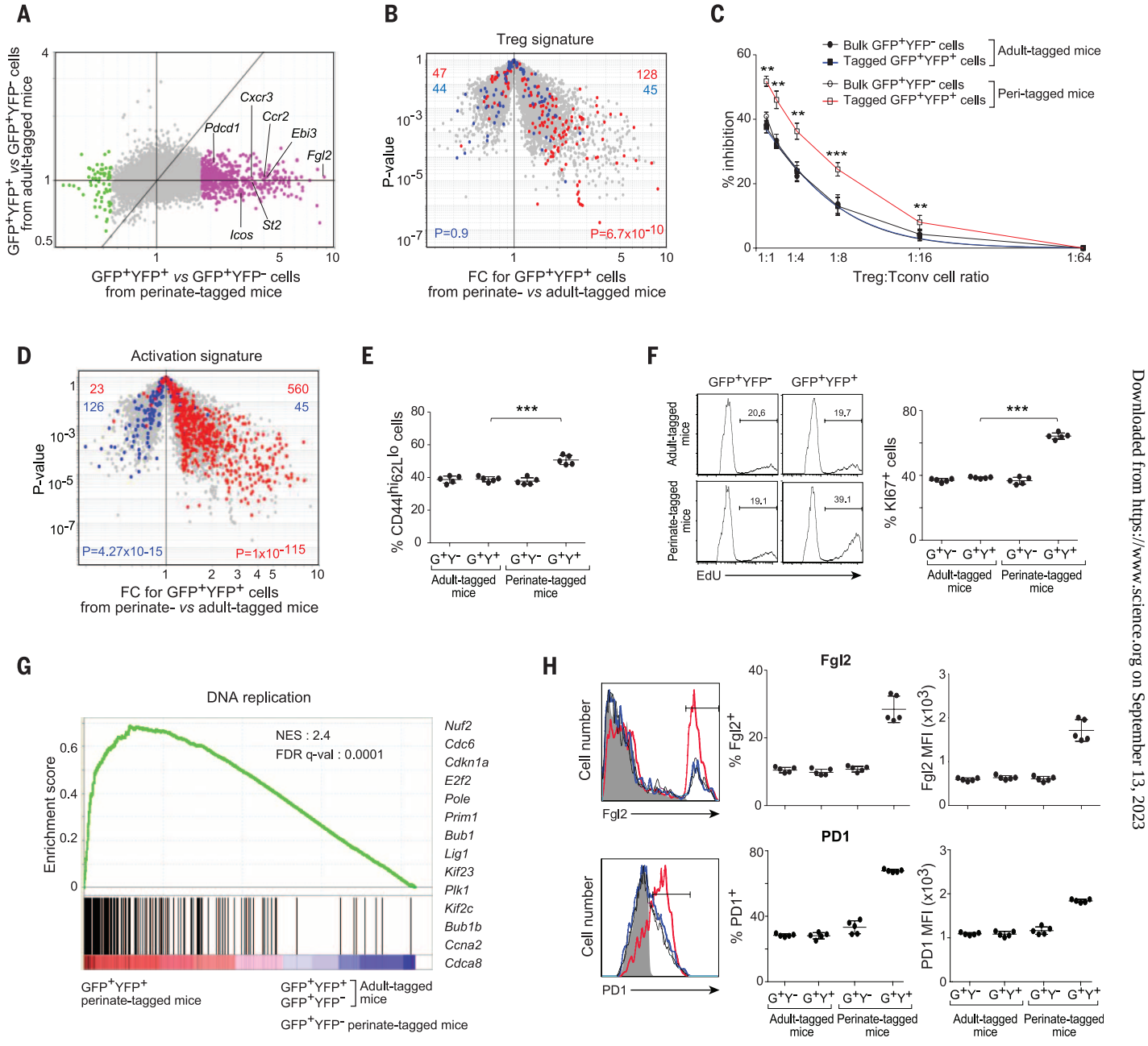

Fig. 3. A distinct transcriptome in perinate-tagged T_{regs}. The same type of four-way comparison used in Fig. 2 was performed except that the sorted cells were analyzed for diverse phenotypic features. (**A**) FC/FC plots comparing perinate-tagged GFP$^+$YFP$^+$ cells versus bulk GFP$^+$YFP$^-$ cells from the same mice (*x* axis) and adult-tagged GFP$^+$YFP$^+$ cells versus bulk GFP$^+$YFP$^-$ cells from the same mice (*y* axis). Pink dots denote transcripts overrepresented in perinate-tagged GFP$^+$YFP$^+$ cells; green dots indicate underrepresented transcripts. (**B**) *P*-value versus FC volcano plot comparing gene expression of perinate-tagged GFP$^+$YFP$^+$ and adult-tagged GFP$^+$YFP$^+$ cells. Red and blue dots indicate up- and down-regulated T_{reg} signature genes, respectively (*31*). *P*-values from the chi-squared test. (**C**) Classical in vitro suppression assay on the four sorted T_{reg} populations. $^{**}P \le 0.01$, $^{***}P \le 0.001$ (Student's *t* test). (**D**) Same volcano plot as in (B), except that up- (red) and down- (blue) regulated activation signature genes (*31*) are superimposed. (**E**) Summary data on late activation marker (CD44^{hi}CD62L^{lo}) expression in the four T_{reg} populations. n = 5. $^{***}P \le 0.001$ (Students' *t* test). (**F**) EdU uptake (left) and Ki67 expression (right) by the four T_{reg} populations. $^{***}P \le 0.001$. (**G**) GSEA of transcripts increased in the perinate-tagged GFP$^+$YFP$^+$ relative to the adult-tagged control T_{reg} populations. NES, normalized enrichment score. FDR q-val, false discovery rate. Representative transcripts showing increased expression are shown on the right. (**H**) Flow cytometric confirmation of gene overexpression in perinate-tagged T_{regs}. For Fgl2 and PD1: Left: representative flow-cytometric histograms; red, perinate-tagged; blue, adult-tagged; black, control bulk populations; gray shading, isotype-control antibody; bar indicates marker positivity. Center: summary data for percentage of the four T_{reg} populations expressing the marker; Right: summary data for marker MFI in the marker-positive population.

Such differences in the Ag processing and presentation machinery of MECs from perinatal and adult mice suggested that their T_{reg} TCR repertoires might diverge. We constrained the inventory of TCRs to be examined by using an approach that had proven fruitful in the past (*21*, *22*). BDC2.5 is a $V_\alpha1^+V_\beta4^+$ T helper cell specificity directed at a pancreatic Ag presented by A^{g7} molecules; hence, generation of T_{regs} in BDC2.5/NOD mice is dependent on rearrangement of an endogenous *Tcra* gene and thymic selection on the resulting second TCRαβ complexes. The fixed $V_\beta4^+$ chain constrains the TCR repertoire, and the analysis is further delimited by sorting individual cells expressing $V_\alpha2$. We sequenced 281 $V_\alpha2^+$ TCR CDR3 regions from splenic T_{regs} of three individual BDC2.5/NOD adults and another 232 from the corresponding population of three individual perinates. This restricted, but parallel, slice of the TCR repertoire was clearly different in the two age groups. Perinate T_{reg} TCRs

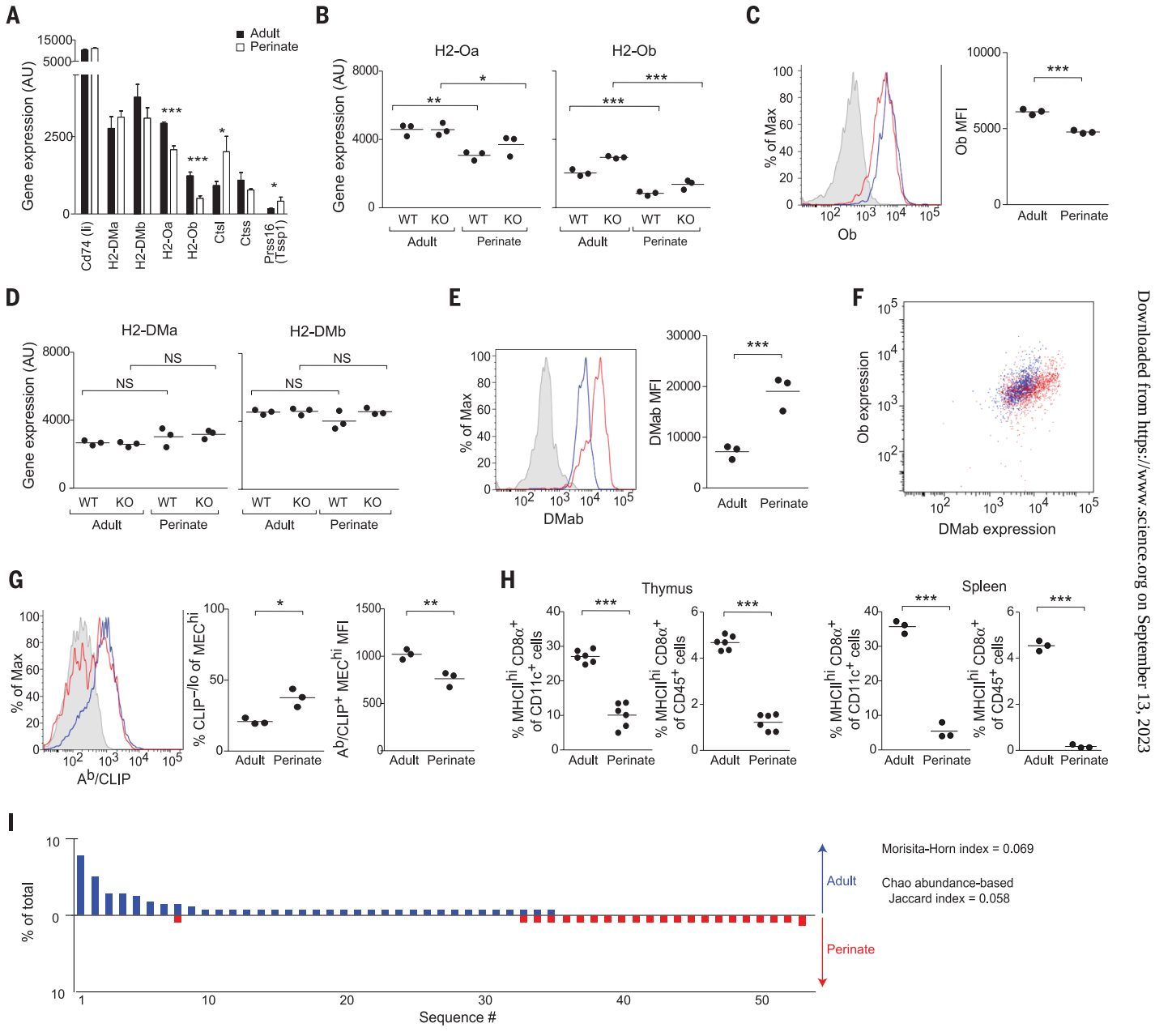

Fig. 4. Age-dependent, Aire-independent differences in the processing and presentation of MEC-generated peptides. (**A**) Microarray-based quantification of transcripts encoding a set of proteins involved in processing and presentation of MHCII-bound peptides. (**B**) Microarray-based quantification of DOa and DOb in MEC^{hi} from *Aire*-WT or -KO adults or perinates. (**C**) Intracellular expression of DOb protein. Left: representative flow-cytometric histograms. Red, perinate; blue, adult; gray shading, negative control staining. Right: summary MFI data. (**D** and **E**) Same as in (B) and (C) except that DMa and DMb were examined. (**F**) Coordinate intracellular staining of DOb and DMab. (**G**) Surface expression of Ab:CLIP complexes on MEC^{hi}. Left: representative flow-cytometric histograms. Red, perinate; blue, adult; gray shading, negative control staining. Center: summary data for percentage of MEC^{hi} expressing little or no CLIP. Right: summary data for MFI. (**H**) Flow cytometric quantification of $MHC^{hi}CD8\alpha^+$ DCs in perinatal versus adult thymus (left) and spleen (right). Summary data for representation in the $CD11c^+$ (left) and $CD45^+$ (right) compartments. (**I**) High-frequency $V\alpha2^+$ TCRs from 5-week-old (upper) and 4-day-old (lower) BDC2.5/NOD females. These sequences correspond to those in table S2. Bars represent frequency of each sequence. (A to H) $^*P < 0.05$, $^{**}P < 0.01$, $^{***}P < 0.001$ (Student's *t* test). *n* = 3 to 6.

were less clonally expanded (fig. S12A), had shorter CDR3α stretches (fig. S12B) and, as expected (*23*), had fewer *Tcra* N-region additions (fig. S12C). To permit a more statistically robust assessment, we focused on repeat sequences. There were many more repeated sequences in the adult mice, and very low values were obtained for both the Morisita-Horn index (0.069 on a scale from 0 to 1) and the Chao abundance-based Jaccard index (0.058 on a scale from 0 to 1), indicating that the two repertoires were very different (table S2 and Fig. 4I).

Thus, our data highlight Aire's ability to promote the generation of a distinct compartment of $Foxp3^+CD4^+$ T_{regs} as the explanation for its importance during the perinatal age window. Given the age-dependent differences in Ag processing machinery and presenting cells that we documented, juvenile and older mice are likely to have distinct repertoires of both Aire-dependent and Aire-independent T_{regs}, selected primarily on Ag:MHC complexes encountered on MECs. These findings add to, rather than negate, Aire's role in clonal deletion of self-reactive thymocytes, established in multiple experimental contexts (*4*, *5*, *24*, *25*).

There are notable similarities in the autoimmune diseases provoked by constitutive genetic ablation of *Aire*, thymectomy at 3 days of age, and perinatal depletion of Foxp3-expressing cells—in particular, the pattern of target tissues on different genetic backgrounds (*26*, *27*) (Fig. 1). Our studies yield a unifying explanation for these phenocopies: The perinatally generated, Aire-dependent T_{reg} compartment is particularly proficient at protecting a defined set of tissues from autoimmune attack, and there may be little overlap with the tissues guarded by adult T_{regs}. This notion is consistent with the observations that mice that underwent a thymectomy 3 days after birth exhibit multiorgan autoimmune disease but do not have a numerically diminished T_{reg} compartment when they get older (*28*, *29*), and that mice constitutively devoid of T_{regs} or inducibly depleted of them as adults show a very different spectrum of pathologies (*9*–*11*). Such a dichotomy could also explain why the autoimmune disease characteristic of both APECED patients and *Aire*-KO mice is restricted to such a limited set of tissues. An important implication of this dichotomy is that therapies based on transfer of T_{regs} isolated from adult donors may not be able to impact a particular subset of autoimmune diseases. Thus, our findings extend the notion of a "layered" immune system (*30*).

REFERENCES AND NOTES

1. K. Aschenbrenner *et al.*, *Nat. Immunol.* **8**, 351–358 (2007).
2. M. Hinterberger *et al.*, *Nat. Immunol.* **11**, 512–519 (2010).
3. S. Malchow *et al.*, *Science* **339**, 1219–1224 (2013).
4. J. S. Perry *et al.*, *Immunity* **41**, 414–426 (2014).
5. R. T. Taniguchi *et al.*, *Proc. Natl. Acad. Sci. U.S.A.* **109**, 7847–7852 (2012).
6. M. Guerau-de-Arellano, M. Martinic, C. Benoist, D. Mathis, *J. Exp. Med.* **206**, 1245–1252 (2009).
7. M. S. Anderson *et al.*, *Immunity* **23**, 227–239 (2005).
8. Materials and methods are available as supplementary materials on *Science* Online.
9. J. D. Fontenot *et al.*, *Immunity* **22**, 329–341 (2005).
10. J. M. Kim, J. P. Rasmussen, A. Y. Rudensky, *Nat. Immunol.* **8**, 191–197 (2007).
11. Z. Chen, C. Benoist, D. Mathis, *Proc. Natl. Acad. Sci. U.S.A.* **102**, 14735–14740 (2005).
12. Y. P. Rubtsov *et al.*, *Science* **329**, 1667–1671 (2010).
13. I. Shalev *et al.*, *J. Immunol.* **180**, 249–260 (2008).
14. L. W. Collison *et al.*, *Nature* **450**, 566–569 (2007).
15. M. J. Polanczyk, C. Hopke, A. A. Vandenbark, H. Offner, *Int. Immunol.* **19**, 337–343 (2007).
16. I. Gotsman *et al.*, *Circulation* **114**, 2047–2055 (2006).
17. F. Jotereau, F. Heuze, V. Salomon-Vie, H. Gascan, *J. Immunol.* **138**, 1026–1030 (1987).
18. J. M. Gardner *et al.*, *Science* **321**, 843–847 (2008).
19. E. D. Mellins, L. J. Stern, *Curr. Opin. Immunol.* **26**, 115–122 (2014).
20. Y. O. Poluektov, A. Kim, S. Sadegh-Nasseri, *Front. Immunol.* **4**, 260 (2013).
21. J. Wong, D. Mathis, C. Benoist, *J. Exp. Med.* **204**, 2039–2045 (2007).
22. J. Nishio, M. Feuerer, J. Wong, D. Mathis, C. Benoist, *J. Exp. Med.* **207**, 1879–1889 (2010).
23. M. Bogue, S. Gilfillan, C. Benoist, D. Mathis, *Proc. Natl. Acad. Sci. U.S.A.* **89**, 11011–11015 (1992).
24. D. Mathis, C. Benoist, *Annu. Rev. Immunol.* **27**, 287–312 (2009).
25. K. Kisand, P. Peterson, *Ann. N. Y. Acad. Sci.* **1246**, 77–91 (2011).
26. W. Jiang, M. S. Anderson, R. Bronson, D. Mathis, C. Benoist, *J. Exp. Med.* **202**, 805–815 (2005).
27. K. S. Tung, Y. Y. Setiady, E. T. Samy, J. Lewis, C. Teuscher, *Curr. Top. Microbiol. Immunol.* **293**, 209–247 (2005).
28. H. C. Dujardin *et al.*, *Proc. Natl. Acad. Sci. U.S.A.* **101**, 14473–14478 (2004).
29. E. T. Samy, K. M. Wheeler, R. J. Roper, C. Teuscher, K. S. Tung, *J. Immunol.* **180**, 4366–4370 (2008).
30. L. A. Herzenberg, L. A. Herzenberg, *Cell* **59**, 953–954 (1989).
31. J. A. Hill *et al.*, *Immunity* **27**, 786–800 (2007).

ACKNOWLEDGMENTS

We thank A. Rudensky, M. Anderson, and A. Lichtman for providing valuable mouse strains; F. Depis and H.-K. Kwon for insightful discussions; and A. Ortiz-Lopez, L. Denu, and K. Hattori for technical assistance. The data presented in this paper are tabulated in the main paper and in the supplementary materials. Microarray data can be found at Gene Expression Omnibus under accession numbers GSE66332 and GSE66402. This work was supported by NIH grant R01 DK060027 (to D.M.). S.Y., N.F., and D.K. were supported by fellowships from the National Research Foundation of Korea (NRF-2013M3A9B6076413), Japan Society for the Promotion of Science, and National Science Foundation, respectively.

SUPPLEMENTARY MATERIALS

www.sciencemag.org/content/348/6234/589/suppl/DC1
Materials and Methods
Figs. S1 to S12
Tables S1 and S2
References (*32*–*42*)

15 January 2015; accepted 4 March 2015
Published online 19 March 2015;
10.1126/science.aaa7017

Regulatory T cells generated early in life play a distinct role in maintaining self-tolerance

Siyoung Yang, Noriyuki Fujikado, Dmitriy Kolodin, Christophe Benoist, and Diane Mathis

Science, **348** (6234), .
DOI: 10.1126/science.aaa7017

Early T cells keep autoimmunity at bay

A major challenge faced by the immune system is to react to foreign substances, such as microbes, while simultaneously tolerating the self. Upsetting this balance leads to autoimmunity. Regulatory T cells (T_{regs}), are a subset of immune cells that help to maintain this balance. Yang *et al.* found that murine T_{reg} cells generated very early in life are distinct from those generated in older animals and play an especially important role in keeping autoimmunity in check (see the Perspective by Tanaka and Sakaguchi). These changes are due to differences in the way T_{regs} develop in the thymus in newborn versus adult mice.

Science, this issue p. 589; see also p. 506